

An Exact Diagonalization Study of the Anisotropic Triangular Lattice Heisenberg Model Using Twisted Boundary Conditions

Mischa Thesberg^{1,*} and Erik S. Sørensen^{1,†}

¹*Department of Physics & Astronomy, McMaster University
1280 Main St. W., Hamilton ON L8S 4M1, Canada.*

(Dated: September 27, 2018)

The anisotropic triangular model, which is believed to describe the materials Cs_2CuCl_4 and Cs_2CuBr_4 , among others, is dominated by incommensurate spiral physics and is thus extremely resistant to numerical analysis on small system sizes. In this paper we use twisted boundary conditions and exact diagonalization techniques to study the phase diagram of this model. With these boundary conditions we are able to extract the inter- and intrachain ordering q -vectors for the $\frac{J'}{J} < 1$ region finding very close agreement with recent DMRG results on much larger systems. Our results suggest a phase transition between a long-range incommensurate spiral ordered phase, and a more subtle phase with short-range spiral correlations with the q -vector describing the incommensurate correlations varying smoothly through the transition. In the latter phase correlations between next-nearest chains exhibits an *extremely* close competition between predominantly antiferromagnetic and ferromagnetic correlations. Further analysis suggests that the antiferromagnetic next-nearest chain correlations may be slightly stronger than the ferromagnetic ones. This difference is found to be slight but in line with previous renormalization group predictions of a collinear antiferromagnetic ordering in this region.

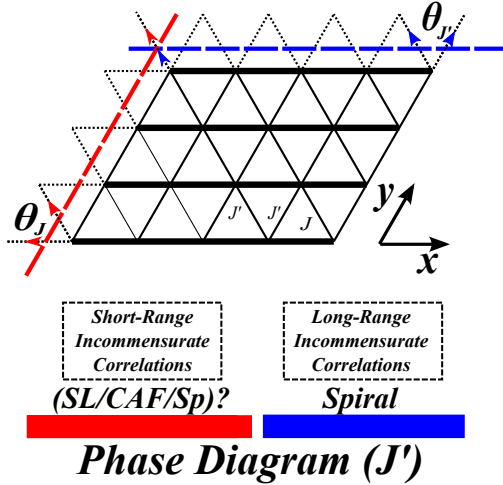


FIG. 1. The anisotropic triangular lattice showing a typical ED cluster. The boundary twists θ_J and $\theta_{J'}$, as discussed in the text, are as shown. The colored arrows indicate the ‘positive’ direction of the twist. The upper leftmost bond receives a twist of $\theta_J + \theta_{J'}$. Below the lattice diagram is a sample phase diagram showing an incommensurate spiral ordering for $J'/J \sim 1$ with a transition to an unknown phase (speculated to be either long-range collinear antiferromagnetically ordered (CAF), short-ranged incommensurate spiral ordered or a two-dimensional spin liquid, among other things).

I. INTRODUCTION

In the study of two-dimensional quantum magnets, the anisotropic triangular model has been a continuing object of attention. This is partially due to its applicability to real experimental materials such as the organic salts $\kappa\text{-(BEDT-TTF)}_2\text{Cu}_2(\text{CN})_3$,¹⁻³ $\kappa\text{-(BEDT-TTF)}_2\text{Cu}_2[\text{N}(\text{CN})_2]$,³ and inorganic Cs_2CuCl_4 ,⁴⁻⁸ and

Cs_2CuBr_4 ,^{8,9} and partially due to early theoretical and numerical speculation that it could exhibit a coveted 2D spin liquid phase.¹⁰⁻¹³ This was followed by suggestions that experimental results on Cs_2CuCl_4 could be explained by, less exotic, quasi-1D spin liquid behaviour.^{14,15} This led to more recent theoretical work, utilizing renormalization group techniques, suggesting a subtle collinear antiferromagnetic (CAF) ordering in this same region;^{16,17} this ordering being in competition with the more classical incommensurate spiral order, which also may exist.¹⁸ Most recently a DMRG study using periodic boundary conditions considered substantially larger systems than before and found a gapped state with strong antiferromagnetic correlations accented by weak, short-range, incommensurate spiral ones.¹⁹

Thus, the question in the $J' \ll J$ region is whether the systems exhibits a one- or two-dimensional spin liquid phase,^{10-13,20} or a collinear antiferromagnetic order driven by next-nearest chain antiferromagnetic correlations and order by disorder,¹⁶ or something entirely different. Suffice it to say that the true physics of this system remains controversial.

Though Dzyaloshinskii-Moriya and interplane interaction are believed to play a role in the physics of the previously mentioned real materials, the more simplified system of a Heisenberg model on a triangular lattice with exchange interactions J along one direction and differing interactions (J') along the other two primitive vectors (see Fig. 1), is believed to capture much of the relevant physics. For $J' < J$ this can be visualized as an array of weakly interacting chains. In the limit of only two chains this system reduces to the well studied $J_1 - J_2$ chain, which is known to be a gapless Luttinger liquid for $J \ll J'$ before undergoing a phase transition at $J \simeq 0.24J'$ to a gapped phase characterized by dimer-like and incommensurate spiral correlations.²¹⁻²⁸ Though it

is known that the behaviour of the true two-dimensional system differs greatly.

In this paper we explore the $J' < J$ region of the anisotropic triangular lattice Heisenberg model (ATLHM) through the use of twisted boundary conditions (TBC) and exact diagonalization (ED). This allows for a minimally biased exploration of the incommensurate behaviour of the system. A typical cluster used in the calculations along with the imposed twists is shown in Fig. 1. By minimizing the total energy of the ground-state with respect to the applied twist we can determine the *optimal twist* θ^{gs} that most closely fit with the natural ordering present in the system. It is then possible to infer a preferred q -vector from the value of the θ^{gs} . The inferred q -vector can tentatively be interpreted as the preferred q -vector for the system in the thermodynamic limit. It is not limited to the usual discrete values $2\pi n/L$ but can take *any* value between 0 and 2π . When such an analysis is performed for the *ground-state* we can directly determine q^{gs} for the ground-state, a substantial advantage of the present approach. We identify non-trivial values of θ^{gs} with the presence of long-range spiral order. Our results seem to indicate a phase transition between two gapless phases: long-range spiral order with a non-trivial ground-state $q^{gs} \neq 0$ and a more subtle phase with $q^{gs} = 0$ and antiferromagnetic intrachain ordering. At the critical point, the minimum in twist-space abruptly jumps between two distinct minima resulting in a similar jump in the inferred q^{gs} . We very roughly estimate this transition to occur at a $J'_c \lesssim 0.5$ in the thermodynamic limit. However, we note that the severe limitation in system sizes when performing exact diagonalizations makes it difficult to draw a definitive conclusion concerning this transition in the thermodynamic limit. The inter-chain correlations of the latter phase are further explored with specific attention paid to the competition between next-nearest chain antiferromagnetic and ferromagnetic correlations as well as nearest chain incommensurate spiral interactions. Our results, though not conclusive, seem to favor a CAF-like ordering in this region. A schematic phase-diagram is shown in Fig. 1.

It is important to realize that the behavior of actual correlation functions are not only determined by q^{gs} . In fact, following Ref. 28, we argue that the dominant part of the incommensurate transverse correlations can be estimated by studying the *first excited state*. In general, q -vectors, describing the *transverse correlations*, are best determined by locating the twist minimizing the energy of the first excited-state. If this minimum is located we can infer a q^1 -vector from which q , describing the incommensurate correlations, can be determined through the relation $q^1 = q + q^{gs}$. It is quite possible to have $q \neq 0$ and thus clear incommensurate (short-range) correlations in the absence of long-range spiral order. Such short-range incommensurate would then typically be modified by an exponentially decaying envelope. Hence, by studying the minima of mainly the first excited-state, we are able to extract the incommensurate q -vectors describing correla-

tions along both the inter- and intrachain directions. Our results for the intrachain q -vector describing the incommensurate correlations are in *very close* agreement with recent DMRG results¹⁹ on substantially larger systems, a strong validation of our approach. Further, the extracted q -vector for the correlations *varies smoothly* with J' through the tentative phase transition described above where q^{gs} abruptly jumps showing that incommensurate correlations are present on either side of the transition.

The organization of this paper is as follows: In section I we introduce the model and its classical phase diagram, this is then followed by an introduction to the twisted boundary conditions used here in section II along with a detailed explanation of how q^{gs} and q are determined. We then show our results in section III along with analysis of the two phases. We conclude in section IV.

A. The Anisotropic Triangular Lattice Heisenberg Model (ATLHM)

The system under consideration, the anisotropic triangular lattice Heisenberg model (ATLHM), is described by the following Hamiltonian:

$$H = J \sum_{\mathbf{x}, \mathbf{y}} \hat{S}_{\mathbf{x}, \mathbf{y}} \hat{S}_{\mathbf{x}-1, \mathbf{y}} + J' \sum_{\mathbf{x}, \mathbf{y}} \hat{S}_{\mathbf{x}, \mathbf{y}} \cdot (\hat{S}_{\mathbf{x}, \mathbf{y}+1} + \hat{S}_{\mathbf{x}-1, \mathbf{y}+1}) \quad (1)$$

where for simplicity of exposition all lattice spacings a are taken to be 1 and where $J > 0$ corresponds to antiferromagnetic interactions. A diagram can be found in Fig. 1. In this paper, we are solely concerned with the $J' < J$ region, particularly the region where $J' \ll J$. For reference, the anisotropy found in Cs_2CuCl_4 is estimated to be $J'/J \sim 0.3$.⁴ Throughout this paper we use the convention that a system of size N is composed of W chains (i.e. width W) of length L and is notated $N = W \times L$.

B. The Classical System

The classical limit case of the ATLHM (i.e. $S \rightarrow \infty$) can be straightforwardly solved.^{29,30} The lowest energy configuration can be determined by positing a spiral solution of the form $\mathbf{S} = S \mathbf{u} e^{-i\mathbf{q} \cdot \mathbf{r}}$. This is identical to a local rotation of the quantization direction at each site which is done in spin-wave theory. The resulting energy expression is then

$$E_{cl}(\mathbf{q}) = J \cos(\mathbf{q}_J) + J' \cos(\mathbf{q}_{J'}) + J' \cos(\mathbf{q}_{J'} - \mathbf{q}_J) \quad (2)$$

where the $\hat{S}_i^z \hat{S}_j^z$ term is neglected since it carries no \mathbf{q} dependence. For $J' < J$ we can find the minimum of Eq. (2) by first treating \mathbf{q}_J as a fixed parameter. In that case it immediately follows that the minimum with respect to $\mathbf{q}_{J'}$ is at $2\mathbf{q}_{J'} = \mathbf{q}_J$. Thus, we get

$$E_{cl}(\mathbf{q}) = J \cos(\mathbf{q}_J) + 2J' \cos\left(\frac{\mathbf{q}_J}{2}\right). \quad (3)$$

The global minimum for $J' < J$ can now be found by minimizing this function with respect to \mathbf{q}_J . Solving with the use of trigonometric identities yields the classical ground-state solutions:

$$\mathbf{q}_J = 2 \arccos\left(-\frac{J'}{2J}\right), \quad \mathbf{q}_{J'} = \arccos\left(-\frac{J'}{2J}\right). \quad (4)$$

However, for the region $J'/J = (0, 1]$ the \mathbf{q}_J solution goes from π to $4\pi/3$, we therefore choose a different solution $\tilde{\mathbf{q}}_J = 2\pi - \mathbf{q}_J$, corresponding to a different choice of branch, which ranges from the more physical π to $2\pi/3$. The $\mathbf{q}_{J'}$ solution needs no such adjustment. Thus the final classical solutions are

$$q_J = 2\pi - 2 \arccos\left(-\frac{J'}{2J}\right), \quad q_{J'} = \arccos\left(-\frac{J'}{2J}\right). \quad (5)$$

where we no longer emphasize q_J and $q_{J'}$ as vectors. In the limit of $J'/J \rightarrow 0$ we find $q_J = \pi$, $q_{J'} = \pi/2$, consistent with antiferromagnetic chains with only perturbative coupling.

II. TWISTED BOUNDARY CONDITIONS

The $J' \leq J$ region of the ATLHM is dominated by both incommensurate spiral ordering and short-range incommensurate spiral correlations. These long-wavelength, incommensurate, correlations present formidable challenges to numerical analysis, since attempts to capture physics with wavelengths of $O(10,000) - O(\infty)$ using a system of length $\sim O(10)$ will undoubtedly be dominated by extreme finite-size effects. Even the most recent 2D DMRG results, allowing for the largest systems, can only probe systems of $L \sim 100$ when at $J' = 0.2$ the wavelength of the spiral correlations is expected to be on the order of 10,000.¹⁹ Thus, it is little wonder that early numerical work produced such disputed results.^{10,11}

Many of these finite-size effects can be successfully mitigated through a careful consideration of the boundary conditions. Previous numerical studies^{10,11,19} on the ATLHM were produced using either open, periodic or mixed boundary conditions. Such boundary conditions will strongly distort the physics of an incommensurate system in favour of an ordering which is commensurate with the system size, only admitting the ordering q -vectors

$$q_n = \frac{2\pi}{L}n$$

where L is the length of the system in a given direction. It is this tendency of them to “lock” a long wavelength structure into a much smaller box that produces such spurious, unphysical, results such as sudden parity transitions (a point to be discussed in greater detail below).^{10,11} Thus to greatly reduce this sort of error our calculations were performed using twisted boundary conditions (TBC).

When using twisted boundary conditions, spin interactions which cross the periodic boundary of the otherwise translationally invariant system become rotated in the $x - y$ plane by an angle θ . This corresponds to the boundary conditions

$$S_{L+1}^- = e^{-i\theta} S_1^-, \quad S_{L+1}^+ = e^{i\theta} S_1^+ \quad (6)$$

or, equivalently,

$$S_L^+ S_1^- \rightarrow S_L^+ S_1^- e^{-i\theta}, \quad S_L^- S_1^+ \rightarrow S_L^- S_1^+ e^{i\theta}. \quad (7)$$

where we simplify the discussion by only discussing one dimension of the system. Generalization to higher dimensions is straightforward although care has to be taken in order to define positive and negative θ consistently when a twist is introduced along several bonds. (See Fig. 1.) Physically, the twist corresponds to a spin current where a(n) \uparrow -spin (\downarrow -spin) acquires an extra phase when traversing the periodic boundary from the left (right). Alternatively, the Heisenberg system can be mapped to one of N_\uparrow fermions with the initial Jordan-Wigner transformation $S_i^+ = c_i^\dagger e^{i\pi \sum_{i < j} c_j^\dagger c_j}$, followed by the gauge U(1) gauge transformation, $c_i^\dagger = f_i^\dagger e^{i\frac{\theta}{L}}$. The interpretation is then of a periodic system, on a ring, of N_\uparrow up spins threaded by a flux θ .

A. $J - J_2$ Spin Chain

For an initially translationally invariant system of linear size L a twist of θ imposed at the boundary can then in general be distributed throughout the system by introducing a twist of θ/L at each bond by performing a non-unitary gauge-transformation. We thereby obtain a model with periodic boundary conditions (PBC). Let us take the well known $J - J_2$ spin chain model as an example:

$$H = J \sum_i \hat{S}_i \cdot \hat{S}_{i+1} + J_2 \sum_i \hat{S}_i \cdot \hat{S}_{i+2}. \quad (8)$$

This model is closely related to the ATLHM and was studied using twisted boundary conditions in Ref. 28 where a twist of θ was introduced at the boundary in the terms coupling sites $[L, 1]$ as well as $[L - 1, 1]$ and $[L, 2]$. We can in this case define a translationally invariant model with the *exact* same energy spectrum if we instead introduce a twist of θ/L at each $[i, i + 1]$ bond along with a twist of $2\theta/L$ at each $[i, i + 2]$ bond. This latter model is now manifestly translationally invariant with periodic boundary conditions and any many-body state can then be characterized by a many-body momentum:

$$\tilde{q} = \frac{2\pi n}{L} \quad n = 0, 1, \dots, L - 1 \quad (9)$$

To be explicit, if T_a denotes the operator translating one lattice spacing a in real space, then $T_a \Psi_{\text{PBC}} =$

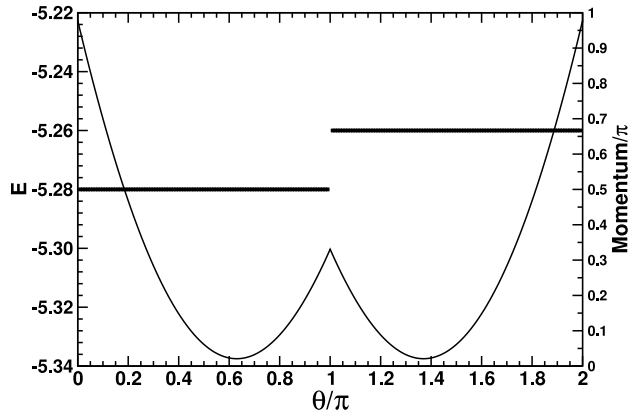


FIG. 2. Energy and momentum of the lowest lying $S = 1$ state for the $J - J_2$ chain at $J_2/J = 1$. The energy minima occur at $\theta = 0.6299\pi, 1.3701\pi$. At $\theta = \pi$ the lowest lying state changes from having $\tilde{q} = 6\pi/12$ to $\tilde{q} = 8\pi/12$.

$\exp(i\tilde{q}a)\Psi_{\text{PBC}}$ with Ψ_{PBC} the wave-function of the translationally invariant model with periodic boundary conditions. We can then determine the energy as a function of θ as well as the many-body momentum of the corresponding state. As an illustration, results are shown in Fig. 2 for the lowest lying $S = 1$ excitation of the $J - J_2$ at $J = J_2$ for a chain with $L = 12$, displaying the characteristic parabolic shape of the energy. In this case the first energy minimum occurs at $\theta_{\text{min}} = 0.6299\pi$ where $\tilde{q} = \pi/2$. We then make the quasi-classical (phenomenological) assumption that the main effect of the twist is to modify the state's natural ordering vector q to fit with the many-body momentum \tilde{q} in the following manner:

$$\tilde{q} = q \pm \frac{\theta}{L} = \frac{2\pi n}{L}. \quad (10)$$

In the present case we immediately find

$$q = \pi/2 + 0.6299\pi/12. \quad (11)$$

The second minimum at $\theta_{\text{min}} = 2\pi - 0.6299\pi$ and $\tilde{q} = 2\pi/3$ yields the same

$$q = 2\pi/3 - (2\pi - 0.6299)/12 = \pi/2 + 0.6299\pi/12. \quad (12)$$

In the thermodynamic limit the natural ordering vector q is then simply given by \tilde{q} and any effects of the twist θ upon the determination of q should be negligible as expressed by Eq. (10). This analysis differs in some details from Ref. 28 but yields essentially identical results for the $J - J_2$ chain.

One may also consider the momentum of the model *without* translational invariance and twisted boundary conditions. In this case we find for the wave-function Ψ_{TBC} the relation $T_a \Psi_{\text{TBC}} = \exp(i\alpha a)\Psi_{\text{TBC}}$ with $\alpha = \tilde{q} + \theta N_\uparrow/L$ where \tilde{q} is the many-body momentum of the

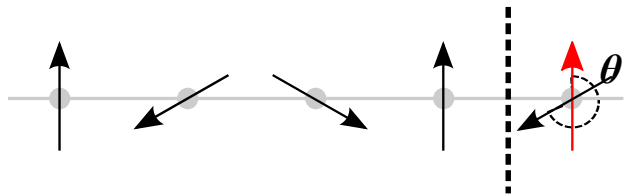


FIG. 3. This diagram shows how a $q = 2\pi/3$ ordering can be made to “fit” into a system of length 4 by twisting by $4\pi/3$ at the boundary. These twisted boundary conditions then allow any incommensurate ordering to fit in any sized system.

translationally invariant system. Here N_\uparrow denotes the number of \uparrow spins in the state under consideration.

If one, at the classical level, argues that θ is the angle needed for qL to equal an integer number of complete turns one arrives at the same relation between q and θ :

$$qL \pm \theta = 2\pi n, \quad (13)$$

In this equation, as well as in Eq. (10), the \pm signifies if q turns in the same direction as θ as we move along the chain. Hence the presence of the twist θ permit a continuum of ordering q -vectors to ‘fit’ into the system of linear size L , where:

$$q = \frac{1}{L} (2\pi n \pm \theta). \quad (14)$$

A simple illustration of this is shown in Fig. 3 for $q = 2\pi/3$. In this case the ordering can be made to “fit” a system of length $L = 4$ if a twist $\theta = 4\pi/3$ is introduced as indicated in Fig. 3. From θ we can then infer $q = (2\pi \times 2 - 4\pi/3)/4 = 2\pi/3$. In this example, the wavelength of the twist ($\lambda = 3$) is shorter than the linear length of the system $L = 4$ and we have to use $n = 2$ in Eq. (14) in order to obtain the correct q . In analogy with the example of the $J - J_2$ chain we would therefore expect the energy minimum for $\theta = 4\pi/3$ to occur for the state with many-body momentum $\tilde{q} = 2\pi \times 2/4 = \pi$. Correspondingly we would expect another minimum at $\theta = 2\pi/3$ for a state with many-body momentum $\tilde{q} = 2\pi/4 = \pi/2$.

In practical studies it is not always feasible to use a translationally invariant system and explicitly determine the many-body \tilde{q} of the state corresponding to the minimizing twist and thereby n in Eq. (10) and (14) and for most of the results presented here we have not done so. However, it is almost always possible to infer the correct n to be used in Eq. (10) and (14) by simple continuity from known results and other expected behavior such as $qL \ll 1$.

B. The ATLHM

We now turn to a discussion of the approach we have taken to apply twisted boundary conditions to the ATLHM. With the analysis of the classical system

in mind, we include *two* twists in our analysis of the ATLHM. The first, θ_J , is associated with a twisted boundary in the J direction. The second, $\theta_{J'}$, is then associated with the boundary in the J' direction (see Fig. 1). With both twists implemented the Hamiltonian becomes:

$$\begin{aligned}
H_\theta &= J \sum_{\mathbf{x}>1, \mathbf{y}} \hat{S}_{\mathbf{x}, \mathbf{y}} \hat{S}_{\mathbf{x}-1, \mathbf{y}} + J' \sum_{\mathbf{x}, \mathbf{y}<W} \hat{S}_{\mathbf{x}, \mathbf{y}} \cdot (\hat{S}_{\mathbf{x}, \mathbf{y}+1} + \hat{S}_{\mathbf{x}-1, \mathbf{y}+1}) \\
&+ \sum_{\mathbf{y}<W} \hat{S}_{1, \mathbf{y}}^+ \cdot (J \hat{S}_{L, \mathbf{y}}^- + J' \hat{S}_{L, \mathbf{y}}^-) e^{i\theta_J} + J' \sum_{\mathbf{x}>1} \hat{S}_{\mathbf{x}, W}^+ \hat{S}_{\mathbf{x}, 1}^- e^{i\theta_{J'}} \\
&+ J' \hat{S}_{1, W}^+ \hat{S}_{L, 1}^- e^{i(\theta_J + \theta_{J'})} + H.c. \\
&+ \sum_{\mathbf{y}<W} \hat{S}_{1, \mathbf{y}}^z \cdot (J \hat{S}_{L, \mathbf{y}}^z + J' \hat{S}_{L, \mathbf{y}}^z) + J' \sum_{\mathbf{x}>1} \hat{S}_{\mathbf{x}, W}^z \hat{S}_{\mathbf{x}, 1}^z e^{i\theta_{J'}}.
\end{aligned} \tag{15}$$

Although this Hamiltonian looks quite cumbersome when written out explicitly, conceptually it is very simple. If a left moving \downarrow -spin traverses, either horizontally or diagonally, the left periodic boundary it is rotated in the $x - y$ plane by θ_J . If an upward moving \downarrow -spin traverses, either vertically or diagonally, the upper periodic boundary it is rotated in the $x - y$ plane by $\theta_{J'}$. If a \downarrow -spin traverses the upper left periodic boundary diagonally, thus crossing both twisted boundaries, it is rotated in the $x - y$ plane by $(\theta_J + \theta_{J'})$. Spins in the bulk as well as the z -component of all spins are unaffected by the boundary.

These twists, which explicitly break the global SU(2) spin symmetry, are identical to a twist of θ_J/L on *each* horizontal and north-west to south-east bond along with a twist of $\theta_{J'}/W$ on *each* south-west to north-east and north-west to south-east bond. The north-west to south-east bonds therefore receive a twist of $\theta_J/L + \theta_{J'}/W$ for a system of dimensions $W \times L$. (See Fig. 1.) If this is done one can work with an equivalent translationally invariant model. However, a twist-per-site approach was found to be less fruitful for such small systems and the explicit SU(2) symmetry breaking will play an important role in forcing a S^z quantization direction which will be discussed below.

It is worth noting that the second twist, $\theta_{J'}$, is rarely (if ever) implemented in studies with twisted boundary conditions. Indeed, most existing numerical studies of the ATLHM fail to consider the possibility of incommensurate *interchain* correlations at all, often enforcing periodic or open boundary conditions in the interchain direction even when other, more elaborate, boundary conditions are used along chains. The parameter $\theta_{J'}$, then, serves as a tool to explore such new physics.

Our complete Hamiltonian, boundary twists included, then has three free parameters: The energy parameter J/J' , the intrachain boundary twist θ_J and the interchain boundary twist $\theta_{J'}$. The numerical task then becomes to explore the two-dimensional landscape $(\theta_J, \theta_{J'})$, at a given J'/J , to find the twists which minimize the ground-state energy. From these twists the q -vectors q_J and $q_{J'}$

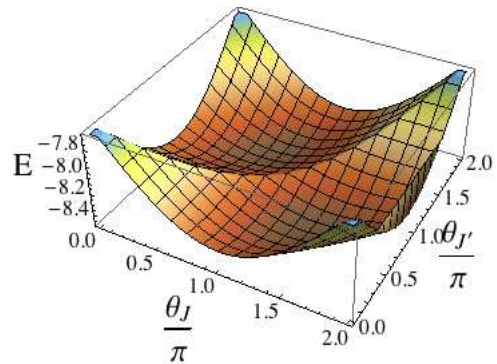


FIG. 4. The energy, E , as a function of the two twists θ_J and $\theta_{J'}$. Results are shown for the lowest-lying $S = 1$ state of a 4×4 system with $J'/J = 1$. The two identical minima occur for $(\theta_J, \theta_{J'}) = (2\pi/3, 4\pi/3)$ and $(4\pi/3, 2\pi/3)$.

can then be extracted using the following generalization of Eq. (10) and (14):

$$\begin{aligned}
q_J &= \vec{q}_1 \cdot \vec{a}_1 = \frac{2\pi n_1}{L} \pm \frac{\theta_J}{L} \\
q_{J'} &= \vec{q}_2 \cdot \vec{a}_2 = \frac{2\pi n_2}{W} \pm \frac{\theta_{J'}}{W}.
\end{aligned} \tag{16}$$

These equations follow since the twists are applied in *direct* space and reflect the behavior of the system upon L and W translations along the directions \vec{a}_1 and \vec{a}_2 in real direct space. Our notation here for a system of W chains of length L is the following: As indicated in Fig. 1 we use basis vectors $\vec{a}_1 = a(1, 0)$ and $\vec{a}_2 = a(1/2, \sqrt{3}/2)$ for the direct lattice. As usual reciprocal lattice vectors are then given by $\vec{b}_1 = 4\pi(\sqrt{3}/2, -1/2)/(a\sqrt{3})$ and $\vec{b}_2 = 4\pi(0, 1)/(a\sqrt{3})$. If we now consider the translationally invariant model with twists of θ_J/L and $\theta_{J'}/W$ along the bonds as described above, the many-body momentum of the translationally invariant system with the imposed twist is:

$$\vec{q} = \frac{n_1}{L} \vec{b}_1 + \frac{n_2}{W} \vec{b}_2. \tag{17}$$

Likewise, in our notation, we have:

$$\vec{q} = \vec{q}_1 + \vec{q}_2 = \frac{q_J}{2\pi} \vec{b}_1 + \frac{q_{J'}}{2\pi} \vec{b}_2. \tag{18}$$

Hence, the application of the twists allow us to determine the components of \vec{q} along \vec{b}_1 and \vec{b}_2 .

As an illustration we show in Fig. 4 results for the $S = 1$ ground-state energy of a 4×4 system with $J'/J = 1$. Two identical minima are clearly present at $(\theta_J, \theta_{J'}) = (2\pi/3, 4\pi/3)$ and $(4\pi/3, 2\pi/3)$. In this case we have done simulations using a translationally invariant model as outlined above and explicitly determined the many-body momentum, \vec{q} , of the state corresponding to the minima. Here we find $(2\pi n_1/L, 2\pi n_2/W) = (\pi/2, \pi)$ and $(\pi, \pi/2)$ respectively. Thus, following the analysis at the end of the previous section we find $q_J = 2\pi/3$. The

mimima in the $S = 0$ ground-state occur at the *exact* same $(\theta_J, \theta_{J'})$ but in this case with $n_1 = n_2 = 0$.

However, there is an additional complication in such an analysis brought on by such small systems. As has very clearly been shown in Ref. 19, much of the $J'/J < 1$ region is dominated by *antiferromagnetic* correlations superimposed on much subtler incommensurate spiral correlations. Thus, if the system can be made to adopt a specific quantization direction z , through, say, a perturbative magnetic field on a single site as was done in Ref. 19, we expect $\langle GS | \hat{S}_{\mathbf{x}}^z \hat{S}_{\mathbf{x}+\mathbf{x}'}^z | GS \rangle$ correlations to be completely dominated by antiferromagnetism with a small canted incommensurate ordering showing in the transverse correlations:

$$\begin{aligned} & \langle GS | \hat{S}_{\mathbf{x}}^x \hat{S}_{\mathbf{x}+\mathbf{x}'}^x + \hat{S}_{\mathbf{x}}^y \hat{S}_{\mathbf{x}+\mathbf{x}'}^y | GS \rangle \\ & \rightarrow \left\langle \frac{1}{2} \left(\hat{S}_{\mathbf{x}}^+ \hat{S}_{\mathbf{x}+\mathbf{x}'}^- + \hat{S}_{\mathbf{x}}^- \hat{S}_{\mathbf{x}+\mathbf{x}'}^+ \right) \right\rangle \propto \langle \hat{S}_{\mathbf{x}}^+ \hat{S}_{\mathbf{x}+\mathbf{x}'}^- \rangle. \end{aligned} \quad (19)$$

In the absence of an explicit symmetry breaking term it is then extremely difficult to separate the spiral correlations from the “sea” of antiferromagnetic ones. This difficulty is addressed by twisted boundary conditions as can be seen through consideration of the following argument, originally detailed and validated in Ref. 28. First, with the addition of a twist in the $x - y$ plane the global spin SU(2) symmetry is broken and a unique z -quantization is picked out in a direction normal to the system, since a generic twist would frustrate antiferromagnetic ordering in-plane. It is then convenient to rewrite the transverse correlations, $\langle \hat{S}_{\mathbf{x}}^+ \hat{S}_{\mathbf{x}+\mathbf{x}'}^- \rangle$, in the more intuitive Fourier transformed form

$$\begin{aligned} & = \left\langle \left(\frac{1}{\sqrt{L}} \sum_{q'} e^{iqx} \hat{S}_{q'}^+ \right) \left(\frac{1}{\sqrt{L}} \sum_q e^{-iq(x+x')} \hat{S}_q^- \right) \right\rangle \\ & = \frac{1}{L} \left\langle e^{-iqx'} \left(e^{i(q-q')x} \right) \hat{S}_{q'}^+ \left(\sum_m |m\rangle \langle m| \right) \hat{S}_q^- \right\rangle \\ & = \frac{1}{L} \sum_q \sum_m e^{-iqx'} |\langle m | S_q^- | GS \rangle|^2 \end{aligned} \quad (20)$$

where S_q^- can now be physically interpreted as a spin-wave destruction operator. If the ground-state lies in the total $S^z = 0$ sector, which it does for an antiferromagnetic system of even system size, then $\langle GS | S_q^- | GS \rangle = \langle GS | \left(\frac{1}{\sqrt{L}} \sum_q e^{-iqx} S_x^- \right) | GS \rangle = 0$ and the transverse correlations can be rewritten as

$$\langle \hat{S}_{\mathbf{x}}^+ \hat{S}_{\mathbf{x}+\mathbf{x}'}^- \rangle = \frac{1}{L} \sum_q \sum_{m \neq GS} e^{-iqr} |\langle m | S_q^- | GS \rangle|^2. \quad (21)$$

As usual, the S_q^- or S_x^- operators take the total $S^z = 0$ ground-state into the total $S^z = -1$ sector. Additionally, if the ground-state has an overall ordering vector q^{gs} then the only terms to survive the sum over $\langle m | S_q^- | GS \rangle$, and thus contribute to the transverse correlations, are those

for which $q^1 = q^{gs} + q$. If one then makes the assumption that only the first excited state in the total $S^z = 1$ sector dominates then one now has a method to extract the incommensurate q -vector, q , as well as the ground-state momentum q^{gs} . First one finds the $(\theta_J, \theta_{J'})$ which minimizes the ground-state energy of the total $S^z = 0$ sector, yielding

$$(q_J^{gs}, q_{J'}^{gs}) \quad (S^z = 0). \quad (22)$$

Notice that our two twists, θ_J and $\theta_{J'}$ yield two q -vectors which we denote q_J and $q_{J'}$. After finding the minimum in the total $S^z = 0$ twist-space the procedure is then repeated in the total $S^z = 1$ twist-space yielding

$$q_J^1 = q_J^{gs} + q_J \quad \text{and} \quad q_{J'}^1 = q_{J'}^{gs} + q_{J'} \quad (S^z = 1). \quad (23)$$

A demonstration of this can be found in Ref. 28. As an illustration of the procedure we show results for $E(\theta_J, \theta_{J'})$ for the first excited state of a 4×6 system with $J'/J = 0.6$ in Fig. 5. Note that, for our subsequent results the minima are determined on a much finer grid. We also note that in both Fig. 4 and 5 do distinct minima occur for values of $\theta > \pi$. This is due to the non-zero $\theta_{J'}$ which lifts the symmetry with respect to $\theta = \pi$ visible in Fig. 2.

This method of minimizing the ground-state energy in both the total $S^z = 0$ and $S^z = 1$ sectors, also allows one to compute the *spin gap*, Δ , between these states. Thus, with knowledge of the spin gap, the ground-state long-range ordering q -vectors as well as the incommensurate short range q -vectors, one can imagine two situations of interest that could arise in the ATLHM.

C. Case 1: $q^{gs} \neq 0$ or π , $q = 0$ (incommensurate spiral order)

In the case where the true ground-state (i.e. that in the total $S^z = 0$ sector) is minimized by incommensurate q -vectors q_J^{gs} and $q_{J'}^{gs}$ we then have incommensurate long-range order related to a classical incommensurate spiral.

In such a region we also expect the spin gap (Δ) to vanish owing to the gapless magnon excitations about the spiral order which accompany U(1) symmetry breaking. Note that the symmetry broken is U(1), since the initial SU(2) symmetry has already been reduced to U(1) when the twist terms were added. This would coincide, in the limit of infinite system size, with long-range correlations of the form

$$\left\langle \hat{S}_{\mathbf{x},\mathbf{y}} \hat{S}_{\mathbf{x}+\mathbf{x}',\mathbf{y}} \right\rangle_{x' \rightarrow \infty} \approx e^{iq_J^{gs} x'} \left\langle \hat{S}_{\mathbf{x}} \right\rangle^2, \quad (24)$$

with a similar form in the J' direction corresponding to $q_{J'}^{gs}$. However, such long-range behaviour of the correlation functions is far beyond the accessible range of any numerical approach. Thus, it will suffice to take a non-zero q^{gs} accompanied by a vanishing spin gap Δ to demonstrate long-range spiral order.

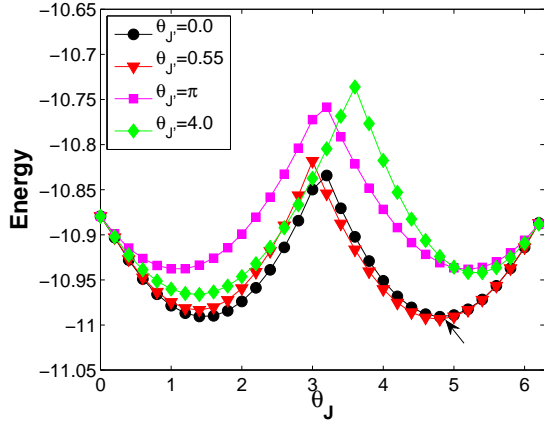


FIG. 5. (Color online.) *Energy* vs. θ_J : The incommensurate and ground-state wavevectors $q_J^{in}/q_{J'}^{in}$ and $q_J^{gs}/q_{J'}^{gs}$ are obtained by minimizing the ground-state energy in the total- $S^z = 1$ and total- $S^z = 0$ subspaces respectively in terms of the boundary twists θ_J and $\theta_{J'}$. This figure shows sample values of θ_J vs. energy for different value of $\theta_{J'}$ for $N = 4 \times 6$ and $J'/J = 0.6$ in the total- $S^z = 1$ subspace. The true minimizing $(\theta_J, \theta_{J'})$ were determined on a much finer grid to an accuracy of 0.001 in the twist, and for this case ($J' = 0.6$) was found to be $(4.775, 0.550)$ (noted by an arrow) which corresponds to the q -vectors $(q_J, q_{J'}) = (2.890, 1.708)$. This figure merely serves as an illustration.

D. Case 2: $q^{gs} = 0$ or π , $q \neq 0$ (non-spiral order)

The case where $q^{gs} = 0$ or π is more complicated. Since q is non-zero the system is displaying incommensurate spiral correlations, however, these correlations are of insufficient strength to stabilize true long-range spiral ordering. Yet, as we find, if the spin gap Δ is found to be zero, then we expect *some* ordering to exist, unless the system is found to be a gapless spin liquid.

Should the value of q^{gs} be consistent with a π ordering vector for all system sizes then, taken along with the gaplessness of the system, one could conclude that the system has ordered antiferromagnetically. However, in our case a more thorough analysis of the correlations of the system becomes necessary. This is expanded upon in Sec. III B

III. RESULTS AND DISCUSSION

The intrachain (θ_J) and interchain ($\theta_{J'}$) boundary twists were varied to minimize the “ground-state” energy in the total- $S^z = 0, 1$ sectors for systems of increasing length and fixed width (4 chains). A fixed width was chosen both since intrachain correlations are the dominant correlations for $J' \ll J$ and to more easily compare with existing DMRG work on larger systems.¹⁹ From these minimizing twist values the q -vectors q_J and $q_{J'}$ were extracted as a function of J'/J which we will simply call

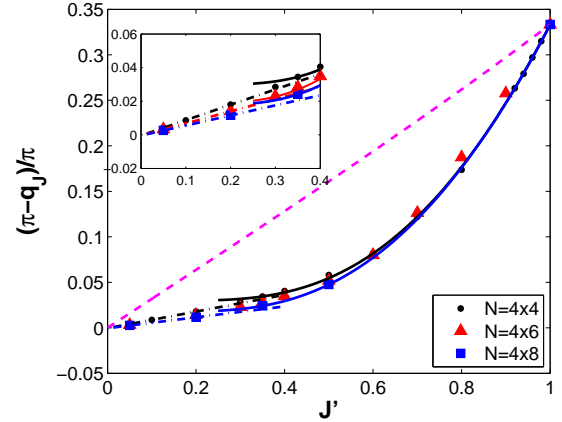


FIG. 6. (Color online.) q_J vs. J' : The intrachain ordering q -vector q_J as a function of the interchain interaction J' for systems of width 4 along with the classical value (dashed magenta line). Results are obtained from the θ_J which minimizes the total- $S^z = 0, 1$ sectors. For $J' > J'_c$ q_J^{gs} was found to be non-zero, while $q_J^{gs} = 0$ or π for $J' < J'_c$. The critical value, J'_c was determined to be $J'_c = 0.9175, 0.7835, 0.7135$ for $N = 4 \times 4, 4 \times 6$ and 4×8 respectively. Exponential fits (black for $N = 4 \times 4$, light grey for $N = 4 \times 6$ and dark grey for $N = 4 \times 8$) are of the form $a(J')^2 \exp(-b/J')$, consistent with Ref. 19, and are found to be extremely good for most of the J' region. However at $J' \sim 0.3$ the data markedly deviates from this fit and develops a linear character. The physicality of this linear behaviour for $J' < 0.3$ is further explored in the text.

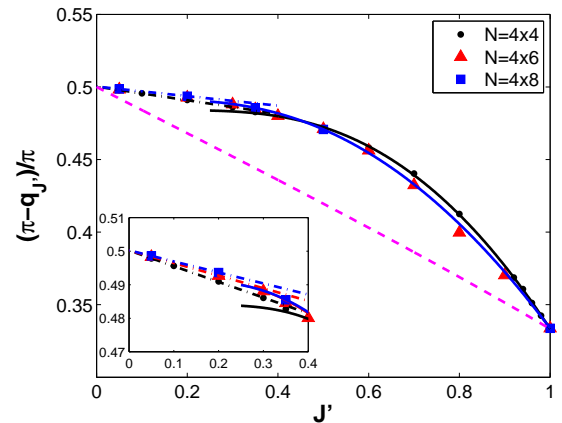


FIG. 7. (Color online.) $q_{J'}$ vs. J' : The interchain ordering q -vector $q_{J'}$ as a function of the interchain interaction J' for systems of width 4. Behaviour and fits are identical to those in Fig. 6. As $J' \rightarrow 0$, $q_{J'}$

J' (i.e. $J = 1$). The resulting data, as well as the classical values, can be found in Fig. 6 for q_J and Fig. 7 for $q_{J'}$. With the exception of the $J' \lesssim 0.3$ region which is discussed later, both q_J and $q_{J'}$ are found to be fitted best by functions of the form $a(J')^2 \exp(-b/J') + c$ rather than power-law fits. This data is in close agree-

ment with the DMRG results found in Ref. 19 where the incommensurate q -vector q_J ($q_{J'}$ was not considered) was extracted by fitting $\langle S_{\mathbf{x}}^z \rangle$, as induced by a boundary field, to an exponentially decaying correlation function of the form $\langle S_{\mathbf{0}}^z \rangle \exp(-x/\xi) \cos(qx)$. The close agreement of our results with the DMRG results on substantially larger systems is surprising and indicative of the power of twisted boundary conditions to circumvent finite-size effects in incommensurate systems.

The lack of distinct features in Fig. 6 and Fig. 7 suggests that the system has identical behaviour for all J' . This is not the case, as can be seen by examining the true ground-state q -vectors in the total- $S^z = 0$ sector. As J' decreases the ground-state twists, θ_J^{qs} and $\theta_{J'}^{qs}$, are found to jump discontinuously at some critical value of J' , J'_c (the nature of this jump will be discussed momentarily). For $J' < J'_c$ the total- $S^z = 0$ and total- $S^z = 1$ twists coincide. Below J'_c the total- $S^z = 0$ data is found to be either 0 or π for all J' in the region. A sample illustration of this jump can be found in Fig. 8 where it is shown for a 4×4 system. This critical value decreases with system size and is found to be at $J'_c = 0.9175, 0.7835, 0.7135$ for $N = 4 \times 4, 4 \times 6$ and 4×8 respectively. A finite-size extrapolation of these values to the thermodynamic limit can be found in Fig. 10. At $J'_c = 0.9175$ the θ_J^{qs} minimizing the energy jumps abruptly to 0 due to the appearance of a new distinct minimum in twist space. We can extrapolate J'_c to the thermodynamic limit with a linear $\frac{a}{N} + b$ fit of N^{-1} estimating $J'_c \rightarrow 0.475$ as $N \rightarrow \infty$. As the system width is increased J'_c is found to increase as well, taking values of 0.912 and 0.917 for systems of size $N = 6 \times 4$ and $N = 8 \times 4$. The infinite system size extrapolation for fixed length, which is obviously non-linear and is thus fitted with a quadratic $\frac{a}{N^2} + \frac{b}{N} + c$ fit, can be found in the inset of 10 and is found to be 0.948. Obviously, for these very limited system sizes, a reliable estimate of the critical coupling in the thermodynamic limit is not within reach. However, it seems plausible that the fixed width estimate of $J'_c = 0.475$ is the more realistic of our estimates. A comparison of both fixed width and fixed length thermodynamic limit extrapolations suggests that the spiral-ordered region extends well into the $J' < J$ region, even in much larger systems.

It is important to note that this discontinuous jump in the ground-state is *not* due to the level crossing observed in previous numerical work.^{10,11} This transition, which was found to be a parity transition, occur for a 4×4 system at a value of $J' \sim 0.84$, for 4×6 and at $J' \sim 0.75$ for 4×8 and thus occurs at a higher value of J' for all system sizes. Thus, this level crossing is completely avoided once one allows the boundaries to twist freely.

The nature of the transition is essentially due to a first-order phase transition in “twist-space” as described by Landau theory. At $J' > J'_c$ the ground-state minima is found to lie at some incommensurate twist value, at $J' \sim J'_c$ a second commensurate minimum forms elsewhere, at say $(\theta_J, \theta_{J'}) = (0, \pi)$, this second minima then lowers in energy as the incommensurate minima, which

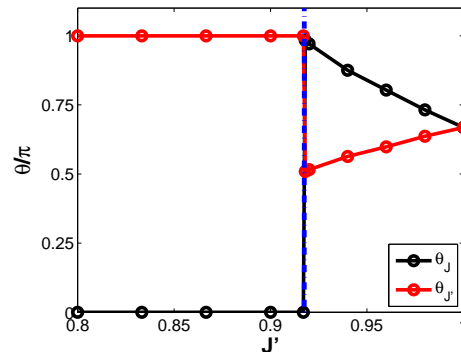


FIG. 8. (Color online.) $\theta_J, \theta_{J'}$ vs. J' in the total $S^z = 0$ subspace ($N = 4 \times 4$): As can be clearly seen the total $S^z = 0$ minimizing boundary twists (shown as solid lines with circular markers) undergoes an abrupt jump (occurring here at $J'/J \sim 0.91$) before “locking” to some fixed value for all $J' < J'_c$.

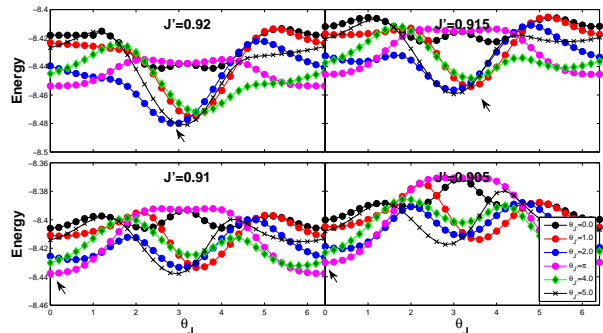


FIG. 9. (Color online.) Energy vs. θ_J for varying values of $\theta_{J'}$, shown for different values of J' near $J'_c = 0.915$ in the total $S^z = 0$ subspace ($N = 4 \times 4$). At $J' > J'_c$ the ground-state minima is found to lie at an incommensurate twist value, at $J' \sim J'_c$ a second commensurate minimum forms at $(\theta_J, \theta_{J'}) = (0, \pi)$, this second minimum then moves lower in energy and becomes the global minimum at $J' = J'_c$. The global minima is indicated in the graphs with an arrow.

is still the global minima, rises. At $J' = J'_c$ the commensurate minimum overtakes the incommensurate one to become the new global minimum and the ground-state then jumps discontinuously.

We now look at each region separately:

A. The Incommensurate Spiral Ordered Phase, $1 \geq J'/J > J'_c/J$

For the isotropic case, where $J' = 1$, the ordering q -vectors $(q_J, q_{J'})$ were found to be $(2\pi/3, 2\pi/3)$ in agreement with previous work. As J' decreases the q -vectors then vary continuously through incommensurate values. In this region the energy minima of the total- $S^z = 0$ and

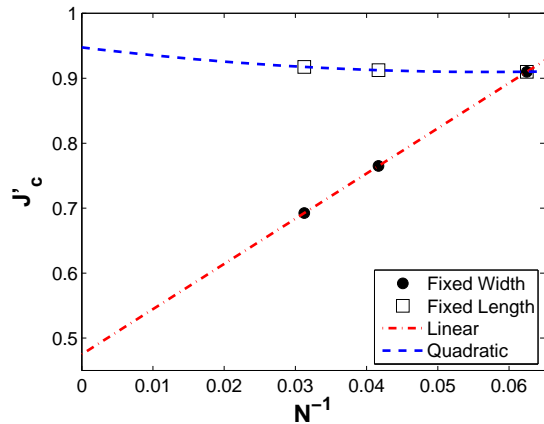


FIG. 10. (Color online.) Critical J' vs N^{-1} : A thermodynamic limit extrapolation of the spiral-ordered to non-spiral ordered transition value (J'_c) for systems of width 4 and length 4. For a width of 4 a linear ($J'_c = 0.475$ as $N \rightarrow \infty$) fit was considered. For a length of 4 the extrapolation was clearly not linear and so a quadratic fit ($J'_c = 0.948$ as $N \rightarrow \infty$) was used. For consistency the quadratic extrapolation values for both analyses are considered the best fit. The critical temperature was indicated by a discontinuous jump in θ_J and $\theta_{J'}$ from their $J' \ll 1$ values.

total- $S^z = 1$ regions coincide in twist space. This, taken with the lack of an energy gap (this is shown in section III B 1), indicates that this region is in a long-range spiral order phase. The transition out of this phase seems to occur at an intrachain twist of $\sim \pi$ for all system sizes as illustrated in Fig. 8 for a 4×4 system. The fact that the transition should be related to some critical value of the boundary twist *and not* some critical q_J is interesting and may represent some subtle numerical cause. However, we would comment that spin wave theory is known to encounter a similar region, notable for its non-convergence, for J' smaller than some critical value^{12,13}. On the other hand, we also cannot exclude the possibility that for much larger systems this transition would be absent.

B. The Non-Spiral Ordered Phase, $J' < J'_c$

For J' values greater than J'_c the ground-state is found to have incommensurate long-range spiral order as was discussed previously. However, for $J' < J'_c$ the twists which minimize the total $S^z = 0$ sector jumps to $(\theta_J, \theta_{J'}) = (0, \pi)$ for $N = 4 \times 4$, 4×6 and 4×8 (i.e. systems of width 4), and to $(0, 0)$ for systems of size $N = 6 \times 4$ and $N = 8 \times 4$. These values of θ_J are found to be entirely consistent with antiferromagnetic intrachain ordering of the ground-state. However, for increasing system width, the values of $\theta_{J'}$, being π for width 4 but 0 for widths of both 6 *and* 8, are inconsistent with any q -vector suggesting a more careful consideration

of interchain physics must be taken. This discussion is postponed until section III B 2.

The fact that no evidence of this transition can be found in the total $S^z = 1$ data suggests that incommensurate correlations are always present and vary smoothly for all $1 > J'/J > 0$, but that the power of those correlations to stabilize long-range spiral order becomes insufficient at J'_c . Below J'_c the dominant correlations are then antiferromagnetic along chains with much smaller incommensurate behaviour resting atop. These antiferromagnetic correlations nested in an incommensurate envelope were demonstrated very clearly for a gapped system in Ref. 19. Though it is our belief that this behaviour is only found below J'_c and the fact that such behaviour was obtained for $1 \geq J'/J > J'_c$ in that paper might be an artefact of the use periodic boundary conditions in the interchain direction there. This point is further discussed in the next subsection.

Numerical access to three system sizes of width 4 makes it possible to extrapolate q_J and $q_{J'}$ to the $4 \times \infty$ limit. Extrapolated values were found to lie, with great precision, on a scaling function of the form $\frac{a}{N^2} + \frac{b}{N} + c$ and can be found in the inset of Fig. 11. The thermodynamic limit results for both q_J^∞ and $q_{J'}^\infty$ are plotted in the main figure. Values above J'_c were not considered, with the exception of the commensurate $J'/J = 1$ case. As before, these q_J^∞ and $q_{J'}^\infty$ data can be well fitted by a function of the form $a(J')^2 \exp(-b/J') + c$. However, unlike the finite-size case, this function is found to be valid for all J' considered. This suggests that the linear behaviour in the neighbourhood of $J' \sim 0$ (See Fig. 6) may not be physical. Furthermore, as will be discussed in section III B 2, it is found for $J' \lesssim 0.3$ that the system's energy dependence on $\theta_{J'}$ becomes zero to numerical precision. Thus it is possible that interchain correlations, which are physically non-zero, but of a magnitude smaller than the smallest number that could be represented by a computer are present in this region. Regardless, the physicality of the linear behaviour is not certain.

1. The Energy Gap: Δ

The numerical determination of a spin gap is in general a difficult task. Often computational reality doesn't permit enough system sizes to be calculated in order for a reliable thermodynamic limit to be established. Furthermore, when the thermodynamic limit can be taken, considerations like the method and boundary conditions used can have a profound effect on the extrapolated results.

With this in mind the bulk of existing numerical work on the ATLHM has suggested the existence of a spin gap either for all of $J'/J < 1$ or for J' less than some critical value in the range of $J'/J \sim 0.6 - 0.8$.^{10,11,19} Indeed, an initial analysis of our own data, as can be seen in the inset of Fig. 12, is consistent with this picture. However, a more careful consideration of these results shows that

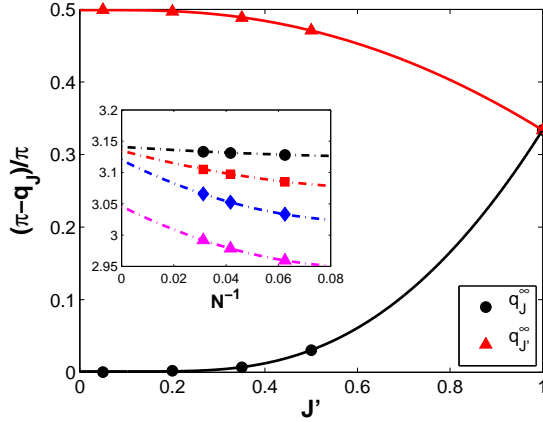


FIG. 11. (Color online.) q_J^∞ and $q_{J'}^\infty$ vs. J' : The thermodynamic limit extrapolated values of q_J and $q_{J'}$ vs. J' . Extrapolations were done to quadratic functions of the form $\frac{a}{N^2} + \frac{b}{N} + c$. Sample extrapolations can be seen in the inset for $J'/J = 0.5$ (triangles), 0.35 (diamonds), 0.2 (squares) and 0.05 (circles). Values greater than the estimated infinite system size transition point and less than $J'/J = 1$ are not shown (see text). In similarity to the finite-size Fig. 6 and Fig. 7, $q_J \rightarrow \pi$ and $q_{J'} \rightarrow \pi/2$ as $J' \rightarrow 0$. However, contrary to that figure, the degradation of an exponential fit to a linear one in the $J' \sim 0$ region is less pronounced, if present at all (see text).

this could be misleading.

As previously, the accessibility of three width 4 system sizes permits a finite-size extrapolation of the energy gap data. This extrapolation was done for values of $J' \leq 0.5$ and can be found in Fig. 12. Values of $1 > J' \geq 0.5$ were not considered due to the possibility of different system sizes being on opposite sides of the J'_c transition. For $J' \leq 0.5$ the Δ values were found to fit very well to a scaling function of form $\frac{a}{N} + \Delta_\infty$ and Δ_∞ was found to be on the order of 10^{-2} . An estimate of the error in this extrapolation can be generated by contrasting the linear fit y-intercept with that of a quadratic fit which produces a Δ_∞ on the order of 10^{-1} . Such small values are extremely suggestive of a gapless system. Taken alone, this is consistent with both spiral and collinear antiferromagnetic orderings as well as potentially a gapless spin liquid phase.

Data was also collected for $J'/J = 1$ where the situation appeared to be different, with linear scaling fits suggesting a small non-zero spin gap. However, it is well known^{31,32} that the spin gap converges very slowly with system size in the spiral-ordered region and the system is known to be gapless in this phase. This, combined with the apparent gaplessness of the $J' < J'_c$ region, suggests that the ATLHM is gapless for all $J'/J \leq 1$.

One of the central results of the numerics of Ref. 19 was the unusual behaviour of the energy gap Δ for different system widths. This paper studied the incommensurate behaviour of long systems of a small number of chains,

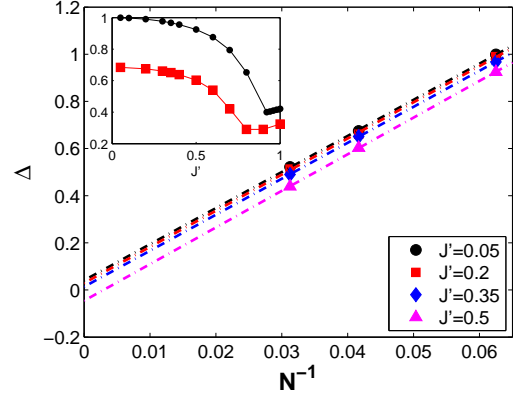


FIG. 12. (Color online.) Spin Gap vs. N^{-1} : The energy difference between the ground-states of the total $S^z = 0$ and total $S^z = 1$ sectors extrapolated to the thermodynamic limit. Dotted lines represent fits of the form $\frac{a}{N} + \Delta_\infty$ with Δ_∞ s found in the non-spiral region to be on the order of 10^{-2} . The error, estimated by contrasting fits quadratic vs. linear in N^{-1} , could be as large as 10^{-1} ; or approximately one percent. Inset: Δ vs. J' : We show the energy gap Δ versus J' for $N = 4 \times 4$ (circles) and $N = 4 \times 6$ (squares). Without a thermodynamic limit analysis it is easy to see how previous work found the $J' < J'_c$ region to be gapped.

i.e. $4 \times 64, 6 \times 64, 8 \times 32$, etc. One of the central results of the paper was that for systems (periodic in \mathbf{y}) of width 2, 4 and 8 the system exhibited a spin gap for $J' < 1$ which shrank with decreasing J' down to $J' \sim 0.5$, the lowest J' studied in the work. This spin gap was accompanied by an exponential decay of intrachain correlations. Conversely, systems of width 6 displayed a small or, likely, no such spin gap and presumably an algebraic decay of correlations. The reason for this discrepancy could not be identified. A possible explanation for the discrepancy between these results and the ones presented here could be the presence of a non-zero $\theta_{J'}$ in our calculations allowing the system to relax more completely as we now comment on in more detail.

For J'/J in the neighbourhood of 1 the classical and quantum ordering vector in the \mathbf{y} direction is $q_{J'} = 2\pi/3$, where for $J'/J \ll 1$ $q_{J'} \rightarrow \pi/2$ as $J' \rightarrow 0$. Thus, a cylinder, as used in Ref. 19, with a width of 6 chains and periodic (no twist) boundary conditions around the cylinder would be commensurate with the $2\pi/3$ order but not the $\pi/2$ order, and thus we expect the correct spin gap for $J'/J \sim 1$ and an artificial, finite size induced gap as J' decreases (though this is not observed in Ref. 19 since the spin gap is only calculated as low as $J' \sim 0.9$ for the 6×64 system). Conversely, system sizes of 4 and 8 are incommensurate with $2\pi/3$ order, and therefore are found to have an unphysical spin gap when $J' \sim J$, but *are* commensurate with a $q_{J'} = \pi/2$ ordering and thus we expect the correct spin gap to emerge as $J' \rightarrow 0$. It is then the case that the 4 and 8 width system would be expected to give the most accurate indication of the

spin gap for small J' and the width 6 system for $J'/J \sim 1$. The key point is that gapless spiral correlations in the J' direction might appear gapped if analyzed with periodic boundary conditions around the cylinder with widths incommensurate with the spiral in that direction. With this in mind, an alternative interpretation of the data of Ref. 19 could be consistent with a system with no spin gap in the thermodynamic limit.

2. Interchain Correlations

Our analysis of intrachain correlations for systems of size 4×4 , 4×6 , 4×8 produced a clear and consistent picture of antiferromagnetically ordered chains ($\theta_J = 0$, $q_J = \pi$ for all chain lengths) accented by incommensurate interchain correlations. The situation for interchain correlations is not so simple.

The open question in the $J' \ll J$ region is whether the systems exhibits a one or two-dimensional spin liquid phase^{10–13} or a collinear antiferromagnetic order driven by next-nearest chain antiferromagnetic correlations and order by disorder¹⁶. This debate can be better informed by a consideration of the interchain ordering vector, $q_{J'}$ and the importance of next-nearest chain antiferromagnetic interactions to the ground-state.

The twist $\theta_{J'}$ which minimizes the ground-state as a function of system *width* is found to be π for 4×4 , and 0 for 6×4 and 8×4 for $J' < J'_c$. This is clearly inconsistent with any classical ordering vector $q_{J'}$. This supports the belief that, for the system sizes under consideration, any long-range classical incommensurate spiral order is suppressed. Previous studies which have shown the lack of long-range spiral order had a potentially critical flaw in that they used periodic boundary conditions which undoubtedly destabilize such orderings. It is then interesting that a lack of spiral order is still found when the system has complete freedom to adopt an incommensurate ground-state.

It is important to remember that, although the long-range incommensurate ordering is suppressed short-range incommensurate correlations are still present. This is manifest by the complete lack of any features of the minimum twist when calculated in the total $S^z = 1$ sector around the critical J'_c . An implication of this is that the short-range behavior of correlation functions would show the same incommensurate behavior above and below J'_c . It is then natural to consider how strong these incommensurate interchain interactions are, and how they compare to the predicted next-nearest chain antiferromagnetic interactions that would drive a CAF ordering.

The strength of interchain correlations can typically be determined by examining $\langle \hat{S}_{\mathbf{x},\mathbf{y}} \hat{S}_{\mathbf{x},\mathbf{y}+y'} \rangle$. However, the value of such an analysis here is hindered by the small system sizes numerically available. This deficiency turns out not to be so significant since the qualitative information relating to the correlation between chains can be

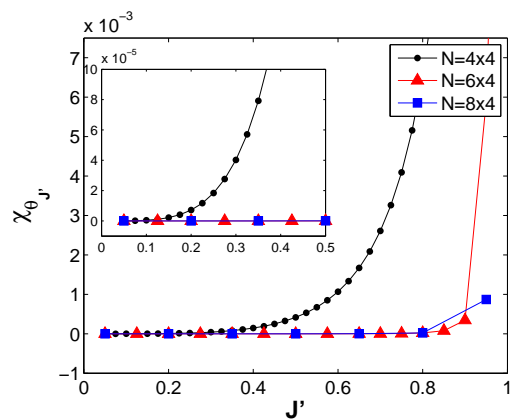


FIG. 13. (Color online.) $\chi_{\theta_{J'}}$ vs. J' : The curvature of the ground-state energy (i.e. total- $S^z = 0$) about its minimum ($\theta_{J'} = \pi$ for $N = 4 \times 4$, $\theta_{J'} = 0$ for $N = 6 \times 4$ and $N = 8 \times 4$) with respect to $\theta_{J'}$ ($\chi_{\theta_{J'}}$) versus J' for systems of increasing width. The size of $\chi_{\theta_{J'}}$ gives an indication of the strength and importance of interchain, (i.e. nearest chain) interactions to the ground-state energy. It is clear that these correlations become smaller with width and become exceedingly weak as $J' \rightarrow 0$. This is consistent with reasoning from RG and the lack of long-range spiral order in this region.

inferred from the curvature of $\theta_{J'}$. For completely decoupled chains the ground-state energy will have no dependence on the interchain twist $\theta_{J'}$, similarly if the minima in $\theta_{J'}$ that minimizes the ground-state energy is found to be extremely shallow then it can be argued that the interchain correlations are extremely weak. Thus, by taking the second numerical derivative, in the total- $S^z = 0$ sector, we can construct a J' -twist susceptibility:

$$\frac{\partial^2 E_{gs}}{(\partial \theta_{J'})^2} = \chi_{\theta_{J'}}. \quad (25)$$

This susceptibility will probe the strength of interchain correlations with a large value of $\chi_{J'}$ representing strong correlations and a small value of $\chi_{J'}$ representing weak ones.

The $\chi_{\theta_{J'}}$ dependence on J' and system width can be seen in Fig. 13 for a $\delta\theta_{J'}$ of 0.1. It can clearly be seen that interchain correlations become tiny as the number of chains increases. In fact the interchain correlations are found to be zero within the 10^{-13} precision of the numerics for systems of width 6 and 8 for small J' even for such a large value of $\delta\theta_{J'}$. This is consistent with the previous claim that these correlations are too weak to force spiral ordering. However, an RG analysis of the ATLHM^{16,17} posit that as the interchain correlations become weak with $J' \rightarrow 0$, the next-nearest chains correlate antiferromagnetically with a strength, J_{nnc} , which grows. We will now consider the effect of such correlations.

Recent series expansion work by Pardini and Singh in Ref. 18 have suggested that an incommensurately ordered ground-state has a lower energy than a CAF one for small J' . However, their work also showed that this

energy difference was extremely small and dependent on how short-ranged spiral correlations are treated. We found previously that the ground-state is not incommensurately ordered for our system sizes for small J' and instead exhibits intrachain antiferromagnetism. A relevant question is then whether the next-nearest chain interactions are antiferromagnetic (CAF) or ferromagnetic (non-CAF or NCAF) and whether these correlations grow as $J' \rightarrow 0$. We previously determined that 6×4 and 8×4 sized systems are minimized, in the total- $S^z = 0$ subspace, by $\theta_{J'} = 0$. This observation makes it difficult to discriminate between CAF and NCAF phases since both would have such a twist. However, the 4×4 system is minimized by a $\theta_{J'} = \pi$, which is inconsistent with CAF ordering. This presents an opportunity to clearly demonstrate the effect of next-nearest neighbour correlations.

We proceed by artificially inserting an exchange coupling between next-nearest chains, $J_{nnn}\hat{S}_{\mathbf{x},\mathbf{y}}\hat{S}_{\mathbf{x}-1,\mathbf{y}+2}$. The question then is, at what strength of J_{nnn} does the 4×4 system adopt a $\theta_{J'} = 0$ ordering (which we take to be CAF). This critical J_{nnn}^c is shown, as a function of J' in Fig. 14. As $J' \rightarrow 0$ the necessary “nudge” the system needs to adopt a CAF ordering becomes very small. In fact, for $J' = 0.05$, this critical interaction strength is as tiny as 0.0003. Contrarily, if a *ferromagnetic* interaction is used (i.e. $J_{nnn} < 0$) then $\theta_{J'}$ does not change, regardless the magnitude of J_{nnn} . The fact that such a minuscule increase in antiferromagnetic next-nearest neighbour correlations can force the ground-state minimizing boundary twist to jump to one consistent with CAF ordering and inconsistent with NCAF ordering lends promise to the notion of CAF ordering in the thermodynamic limit.

The ability to easily force a 4×4 system into a CAF consistent ordering is appealing, but hardly conclusive, evidence that CAF ordering will occur for larger systems, especially since this system is so small. We therefore consider another means of analysing these interactions that can be applied to larger systems.

We begin by perturbing our system with two different arrangements of staggered magnetic field. The first arrangement is chosen to be consistent with CAF ordering and involves antiferromagnetic staggering along chains and between next-nearest chains (see Fig. 15, left). We only apply fields to *every other* chain in order to allow the system the freedom to adopt the classical $q_{J'} = \pi/2$ ordering. The second arrangement is designed to be consistent with ferromagnetic ordering between next-nearest chains (see Fig. 15, right) but still antiferromagnetic along chains. Two susceptibilities are constructed from this perturbation.

The first susceptibility, which we call χ_{NNN} , is constructed from the next-nearest neighbour chain correlation functions:

$$\chi_{NNN} = \frac{\delta^2 \langle \hat{S}_{\mathbf{x},\mathbf{y}} \hat{S}_{\mathbf{x}-1,\mathbf{y}+2} \rangle}{\delta h^2} \quad (26)$$

where h is arranged in one of the two (CAF or NCAF)

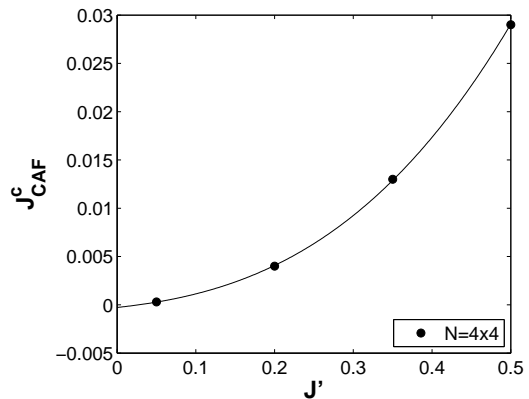


FIG. 14. (Color online.) J_{CAF}^c vs. J' for $N = 4 \times 4$: As is discussed in the text, the $N = 4 \times 4$ system, whose $\theta_{J'}$ of π is found to be incompatible with the predicted collinear-antiferromagnetic (CAF) ordering for $J' \ll 1$, can be forced to a $\theta_{J'}$ of 0, consistent with this ordering by applying only a small next-nearest neighbour antiferromagnetic interaction J_{CAF} (see text). Thus, as a demonstration of the subtle importance of these next-nearest chain interactions the critical J_{CAF}^c for which $\theta_{J'}$ jumps from π to 0 is plotted as a function of J' . For $J' = 0.05$ this value becomes as low as $J_{CAF}^c = 0.0003$ representing an extreme susceptibility to such interactions. Conversely a next-nearest chain *ferromagnetic* interaction is found to have no effect on $\theta_{J'}$. This suggests a strong preference for CAF order. This solid line is given as an aid for the eye.

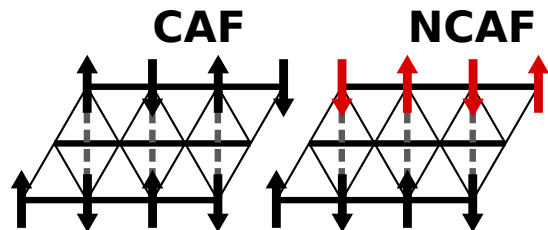


FIG. 15. A diagram of the staggered fields applied in the generation of χ_{NNN} , χ_{CAF} and χ_{NCAF} . The field terms, $h\hat{S}_i^z$, are represented by arrows. Fields are placed on every *other* chain to allow the system freedom to adopt a classical $q_{J'} = \pi/2$ ordering. The collinear antiferromagnetic (CAF) ordering is found on the left and corresponds to antiferromagnetic correlations between next-nearest chains. For clarity, a sample next-nearest chain partner for the non-skewed triangular system is illustrated with a dotted line. The non-collinear antiferromagnetic (NCAF) ordering, corresponding to *ferromagnetic* next-nearest chain correlations, is shown on the right.

ways. The first derivative term was found to be zero, which could have been predicted on the basis of spin inversion symmetry, and thus calculating this quantity is a simple matter of numerical differentiation. The results, as a function of J' , are shown in Fig. 16 where calculations were done only between chains that received a magnetic field (i.e. between chains 0 and 2 or 2 and 4

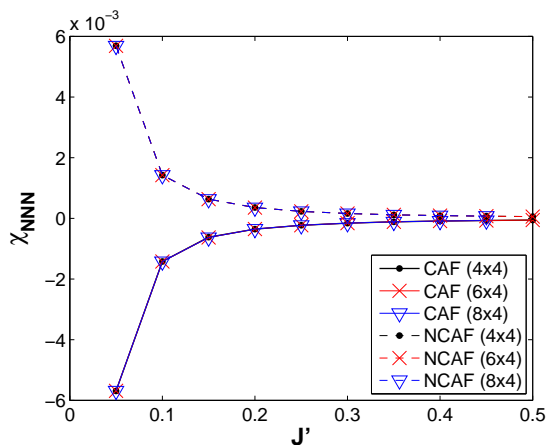


FIG. 16. (Color online.) χ_{NNN} vs. J' and System Size: χ_{NNN} , being a susceptibility of the next-nearest chain correlation function to collinear (CAF) and non-collinear (NCAF) perturbative magnetic fields further discussed in the text, plotted against J' for various system widths. The perturbing field was of strength $h = 0.001$ and applied to half the sites for both CAF and NCAF (see text). Calculations were done in total- $S^z = 0$ about the $\theta_{J'} = 0$ minima. This quantity is found to be largely system size independent and negative (positive) for CAF (NCAF) correlations. This is consistent with the notion that a perturbative CAF field will cause the next-nearest chain correlations to grow more negative and a NCAF field to grow more positive. The extremely similar magnitude of the two correlations suggest the system exhibits a delicate competition between collinear and non-collinear next-nearest chain correlations in the non-spiral ordered phase and that this susceptibility grows as $J' \rightarrow 0$.

but not 1 and 3). The specific chain considered and the specific spin within that chain was found to be irrelevant.

This χ_{NNN} is found to be largely system size independent and negative (positive) for CAF (NCAF) correlations. This is consistent with the notion that a perturbative CAF field will cause the next-nearest chain correlations to grow more negative and a NCAF field to grow more positive. The extremely similar magnitude of the two correlations suggests the system exhibits a delicate competition between collinear and non-collinear next-nearest chain correlations in the non-spiral ordered phase and that this susceptibility grows as $J' \rightarrow 0$. The growth of this susceptibility, coupled with the diminution of nearest-chain correlations as demonstrated in Fig. 13 seems consistent with the picture painted by renormalization theory. However, the system seems potentially equally susceptible to ferromagnetic next-nearest chain interactions. One then wonders which of these correlations ultimately prevails. In order to consider this we consider yet another susceptibility.

To quantify the systems preference towards ferromagnetic versus antiferromagnetic next-nearest chain ordering, we considered the effect that perturbing magnetic fields of Fig. 15 have on the ground-state energy. We

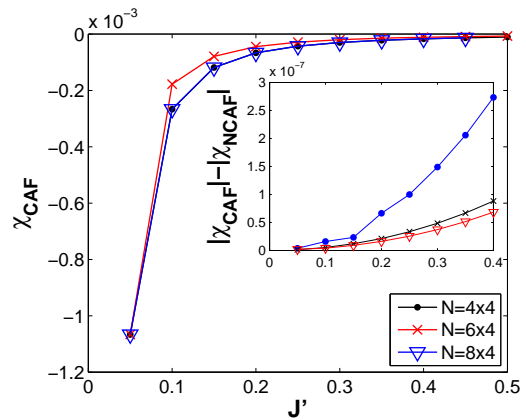


FIG. 17. (Color online.) χ_{CAF} vs. J' : χ_{CAF} , being the second derivative of the ground-state energy (i.e. total- $S^z = 0$, $\theta_{J'} = 0$) with respect to a collinear antiferromagnetic (CAF) perturbing magnetic field, versus J' for systems of varying width. For all system sizes the quantity is found to be negative and increasing in magnitude with decreasing J' . This implies that the system's energy is lowered by promoting CAF-like ordering. In order to establish the strength of this affinity for CAF order vs. non-collinear antiferromagnetic (NCAF) order, a similar ground-state susceptibility is defined relative to an NCAF perturbing magnetic field (χ_{NCAF}). The inset show the difference in magnitude between χ_{CAF} and χ_{NCAF} . χ_{CAF} is found to be greater for all system sizes and J' though only by $\sim 10^{-7}$.

thus define:

$$\chi_{CAF} = \frac{\delta^2 E_{gs}}{\delta h_{CAF}^2}, \quad \chi_{NCAF} = \frac{\delta^2 E_{gs}}{\delta h_{NCAF}^2}. \quad (27)$$

As before, the first derivative term was found to be zero. This is due to spin inversion symmetry. χ_{CAF} can be found plotted in Fig. 17. χ_{NCAF} , which is not plotted, behaves identically except being positive. The fact that χ_{CAF} is negative implies that CAF-ordering lowers the systems energy where NCAF, having a positive χ_{NCAF} , increases it. Furthermore, when we compare the *magnitudes* of the two susceptibilities, which can be found in the inset of Fig. 17, we see that χ_{CAF} is in fact larger than χ_{NCAF} for all system sizes. Though it is important to note that it is only larger by a margin of $\sim 10^{-7}$, and decreases with system width, further evidencing the tenuousness of these competing correlations.

IV. CONCLUSION AND SUMMARY

In this paper we have demonstrated the power of twist boundary conditions to mitigate potentially disastrous finite-size effects in incommensurate systems. Using these twisted boundary conditions we were able to extract the intrachain incommensurate q -vector q_J and found it to be in good agreement with results on substantially larger systems. Furthermore, we were also able

to extract the *interchain* incommensurate q -vector q_J . To our knowledge our is the first work to allow fully incommensurate behaviour in both intra- and interchain directions.

Analysis of the incommensurability in both the ground-state and total $S^z = 1$ excited state revealed a potential phase transition between a long-range spiral ordered phase and one with short-range spiral correlations. A scaling analysis of this critical J'_c suggests that this point is at $J'_c \sim 0.475$ for systems of width 4 and ~ 0.948 for systems of infinite width (length 4). We then attempted to characterize the $J' < J'_c$ phase. We believe it to be gapless in the thermodynamic limit, as well as dominated by both next-nearest ferromagnetic and antiferromagnetic correlations. Additionally, the nearest chain correlations are found to become minuscule. Fur-

ther analysis reveals that the antiferromagnetic interactions are marginally stronger in the systems considered. This is consistent with the renormalization group claim that this region should be CAF ordered.

ACKNOWLEDGMENTS

We would like to thank Sedigh Ghamari, Sung-Sik Lee and Catherine Kallin for many fruitful discussions. We also acknowledge computing time at the Shared Hierarchical Academic Research Computing Network (SHARCNET:www.sharcnet.ca) and research support from NSERC.

* thesbeme@mcmaster.ca

† sorensen@mcmaster.ca; <http://comp-phys.mcmaster.ca>

¹ Y. Shimizu, K. Miyagawa, K. Kanoda, M. Maesato, and G. Saito, Phys. Rev. Lett. **91**, 107001 (2003).

² Y. Qi, C. Xu, and S. Sachdev, Phys. Rev. Lett. **102**, 176401 (2009).

³ H. C. Kandpal, I. Opahle, Y.-Z. Zhang, H. O. Jeschke, and R. Valentí, Phys. Rev. Lett. **103**, 067004 (2009).

⁴ R. Coldea, D. A. Tennant, A. M. Tsvelik, and Z. Tylczynski, Phys. Rev. Lett. **86**, 1335 (2001).

⁵ O. A. Starykh, H. Katsura, and L. Balents, Phys. Rev. B **82**, 014421 (2010).

⁶ R. Coldea, D. A. Tennant, R. A. Cowley, D. F. McMorrow, B. Dorner, and Z. Tylczynski, Phys. Rev. Lett. **79**, 151 (1997).

⁷ R. Coldea, D. A. Tennant, K. Habicht, P. Smeibidl, C. Wolters, and Z. Tylczynski, Phys. Rev. Lett. **88**, 137203 (2002).

⁸ W. Zheng, R. R. P. Singh, R. H. McKenzie, and R. Coldea, Phys. Rev. B **71**, 134422 (2005).

⁹ H. Tanaka, T. Ono, H. A. Katori, H. Mitamura, F. Ishikawa, and T. Goto, Progress of Theoretical Physics Supplement **145**, 101 (2002), <http://ptps.oxfordjournals.org/content/145/101.full.pdf+html>.

¹⁰ M. Q. Weng, D. N. Sheng, Z. Y. Weng, and R. J. Bursill, Phys. Rev. B **74**, 012407 (2006).

¹¹ D. Heidarian, S. Sorella, and F. Becca, Phys. Rev. B **80**, 012404 (2009).

¹² P. Hauke, Phys. Rev. B **87**, 014415 (2013).

¹³ J. Merino, R. H. McKenzie, J. B. Marston, and C. H. Chung, Journal of Physics: Condensed Matter **11**, 2965 (1999).

¹⁴ M. Kohno, L. Balents, and O. Starykh,

Journal of Physics: Conference Series **145**, 012062 (2009).

¹⁵ L. Balents, Nature **464**, 199 (2010).

¹⁶ O. A. Starykh and L. Balents, Phys. Rev. Lett. **98**, 077205 (2007).

¹⁷ S. Ghamari, C. Kallin, S.-S. Lee, and E. S. Sørensen, Phys. Rev. B **84**, 174415 (2011).

¹⁸ T. Pardini and R. P. Singh, Phys. Rev. B **77**, 214433 (2008).

¹⁹ A. Weichselbaum and S. R. White, Phys. Rev. B **84**, 245130 (2011).

²⁰ J. Reuther and R. Thomale, Phys. Rev. B **83**, 024402 (2011).

²¹ M. Thesberg and E. S. Sørensen, Phys. Rev. B **84**, 224435 (2011).

²² S. Chen, L. Wang, S.-J. Gu, and Y. Wang, Phys. Rev. E **76**, 061108 (2007).

²³ T. Tonegawa and I. Harada, J. Phys. Soc. Jpn. **56**, 2153 (1987).

²⁴ S. Eggert, Phys. Rev. B **54**, R9612 (1996).

²⁵ R. Chitra, S. Pati, H. R. Krishnamurthy, D. Sen, and S. Ramasesha, Phys. Rev. B **52**, 6581 (1995).

²⁶ S. R. White and I. Affleck, Phys. Rev. B **54**, 9862 (1996).

²⁷ F. D. M. Haldane, Phys. Rev. B **25**, 4925 (1982).

²⁸ A. A. Aligia, C. D. Batista, and F. H. L. Eßler, Phys. Rev. B **62**, 3259 (2000).

²⁹ A. Yoshimori, Journal of the Physical Society of Japan **14**, 807 (1959).

³⁰ J. Villain, Journal of Physics and Chemistry of Solids **11**, 303 (1959).

³¹ L. Capriotti, A. E. Trumper, and S. Sorella, Phys. Rev. Lett. **82**, 3899 (1999).

³² A. E. Trumper, L. Capriotti, and S. Sorella, Phys. Rev. B **61**, 11529 (2000).